SATELLITE LAUNCHER ON-OFF CONTROLLER FOR ATTITUDE TRACKING AND DECOUPLING

Alvaro P. Oliva **W. C. Leite Filho**
Instituto de Aeronáutica e Espaço (IAE) - Divisão de Sistemas Espaciais
12228-904, São José dos Campos, SP - Brasil
e-mail: oliva@directnet.com.br

Abstract: A study about an on-off satellite launcher control law design for attitude tracking and decoupling was carried out. The study considered a linear decoupled and a linear coupled model of the vehicle to obtain the controller gains. The performance given by each design was assessed. The stability analysis of both designs was also carried out using the describing function technique and the circle criterion. Finally the robustness of the design based on the coupled model was assessed with respect to uncertainties on the control forces and on the inertial parameters. It was assumed that the vehicle is flying a ballistic phase outside the atmosphere.

Keywords: Flight Control Law, On-Off Controller, Tracking, Decoupling.

1 INTRODUCTION

The research concerning the design of an on-off controller for a satellite launcher vehicle is a very useful. This kind of controller is very much used in the non-propulsive phases of the flight. This controller is also used in the propulsive phases for roll control. In this work the case of non-propulsive flight is addressed. The study was concerned with three on-off controllers, one for each mode, that is, pitch, yaw and roll. The controller function is to track a reference attitude and also to decouple the vehicle response. A design study was carried out for an on-off controller of a relay type witch includes a dead zone and without hysteresis in the control system loop. The performance of the vehicle working with this controller was assessed with respect to tracking, coupling, stability, and robustness with respect to uncertainties into the control forces and uncertainties into the vehicle inertial parameters. The analysis of non-linear systems with a relay type can be found, for example, in Gibson (1963), Isidori (1985) and Atherton (1975). Some particular applications for Aerospace cases are reported in Boyle & Brogan (1986), Brumann & Rugh (1986), Hughes (1986) and Bryson (1994). The controller structure here used is not the usual. Most frequently this kind of manoeuvre is performed one by one. The vehicle uses a controller that, for example, first manoeuvres only in the pitch plane, than only in the yaw plane and finally only in the roll plane. The proposed structure here allows the vehicle to manoeuvre in the three planes simultaneously.

So this is a preliminary study to evaluate the problems and advantages of this controller.

Artigo Submetido em 05/05/00
1a. Revisão em 29/08/00; 2a. Revisão em 03/09/01
Aceito sob recomendação do Ed. Consultor Prof. Dr. Liu Hsu

2 VEHICLE DYNAMIC MATHEMATICAL MODELS

Here the vehicle general non-linear model used for this research is described. Based on this non-linear model both linear models are derived. First the linear coupled model and second the linear decoupled model.

2.1 Non-linear Model

The mathematical model of the vehicle dynamics is described by the following six differential equations

$$\dot{p} = \frac{M_\phi}{I_{xx}}\delta_r - \frac{(I_{zz} - I_{yy})}{I_{xx}}qr \tag{1}$$

$$\dot{q} = \frac{M_\theta}{I_{yy}}\delta_z - \frac{(I_{xx} - I_{zz})}{I_{yy}}pr \tag{2}$$

$$\dot{r} = \frac{M_\psi}{I_{zz}}\delta_y - \frac{(I_{yy} - I_{xx})}{I_{zz}}pq \tag{3}$$

$$\dot{\phi} = p - (tg\,\psi\cos\phi)q + (tg\,\psi sin\phi)r \tag{4}$$

$$\dot{\psi} = (sin\phi)q + (\cos\phi)r \tag{5}$$

$$\dot{\theta} = \frac{\cos\phi}{\cos\psi}q - \frac{sin\phi}{\cos\psi}r \tag{6}$$

that can be found on several classical texts, as Greensite (1970), for example.

In figure 1 the vehicle is shown with the angular velocities and angular attitudes described by equations 1 to 6.

As it can be noticed there are no aerodynamic forces or moments in the equations, since the vehicle is studied in the phase outside the atmosphere. It can also be noticed that only the rotational equations were used, since it was considered that

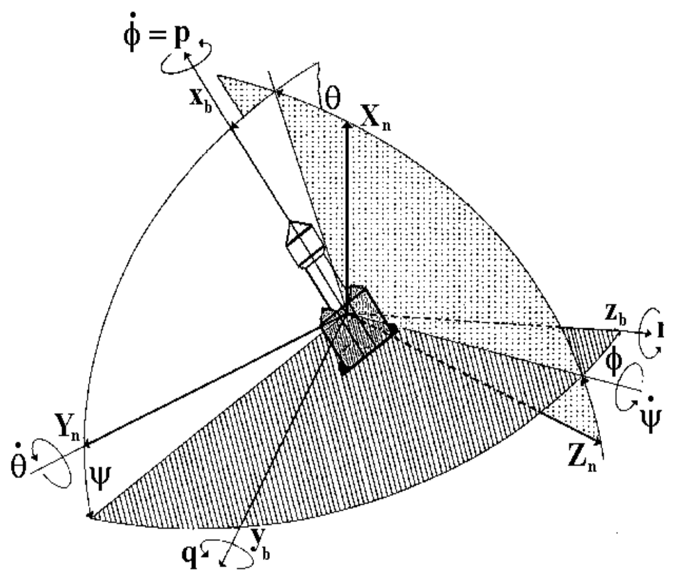

Figure 1 - Satellite Launcher with the corresponding angular velocities and angular attitudes.

the vehicle is flying a ballistic phase, that is, without propulsion. So there is no aerodynamic coupling effect actuating on the vehicle, only inertial coupling and non-linear velocities cross coupling.

In these equations, the meaning of the symbols used for the parameters are the following:

I_{xx}, I_{yy}, I_{zz} moments of inertia with respect to the x, y and z axis, respectively.

M_θ , M_ψ , M_ϕ Control Moments in pitch, yaw and roll respectively.

and for the states:

p perturbation angular velocity about x-body axis (roll rate)

q perturbation angular velocity about y-body axis (pitch rate)

r perturbation angular velocity about z-body axis (yaw rate)

θ perturbation attitude angle in pitch

ψ perturbation attitude angle in yaw

ϕ perturbation attitude angle in roll (bank angle)

δ_z, δ_y, δ_r Actuation signal for the Control Moments in pitch, yaw and roll respectively.

The actuation signals will be discrete values, that is, -1 , 0 or 1 , following the control law design logic. In other words they will be the relay output. It is also useful to mention that equation (4) can be used without any problem here. The problem here addressed is for a vehicle that performs limited manoeuvres in yaw. The example vehicle, the Brazilian Satellite Launcher Vehicle (VLS), has the yaw range limited, and it is quite usual for this kind of vehicle this limitation. For the case addressed $|\psi| \leq 80°$.

2.2 Linear Coupled Model

It is possible to notice that the vehicle model is non-linear and coupled. So, to design the control law it is convenient to use a linear model, in that case it can be used a linear coupled model and a linear decoupled model. The linear coupled model can be described by the following equations,

$$\dot p = -\frac{(I_{zz}-I_{yy})}{I_{xx}}[r_0 q + q_0 r] + \frac{M_\phi}{I_{xx}}\delta_r \quad (1\text{-A})$$

$$\dot q = -\frac{(I_{xx}-I_{zz})}{I_{yy}}[r_0 p + p_0 r] + \frac{M_\theta}{I_{yy}}\delta_z \quad (2\text{-A})$$

$$\dot r = -\frac{(I_{yy}-I_{xx})}{I_{zz}}[q_0 p + p_0 q] + \frac{M_\psi}{I_{zz}}\delta_y \quad (3\text{-A})$$

$$\dot\phi = p-(tg\psi_0\cos\phi_0)q+(tg\psi_0\sin\phi_0)r+ [(r_0\cos\phi_0+q_0\sin\phi_0)tg\psi_0]\phi+ \frac{(r_0\sin\phi_0-q_0\cos\phi_0)}{\cos^2\psi_0}\psi \quad (4\text{-A})$$

$$\dot\psi = (\sin\phi_0)q+(\cos\phi_0)r+(q_0\cos\phi_0-r_0\sin\phi_0)\phi \quad (5\text{-A})$$

$$\dot\theta = \frac{\cos\phi_0}{\cos\psi_0}q - \frac{\sin\phi_0}{\cos\psi_0}r - \frac{(q_0\sin\phi_0+r_0\cos\phi_0)}{\cos\psi_0}\phi + \frac{\sin\psi_0}{\cos^2\psi_0}(q_0\cos\phi_0-r_0\sin\phi_0)\psi \quad (6\text{-A})$$

In this model it is possible to drop out the terms that multiply ϕ and ψ in equations (4-A), (5-A) and (6-A), since for the analysed case, the coefficients of these terms are small when compared with the coefficients that multiply the terms in *p*, *q* and *r*. For a typical flight condition, as shown in tables 1 and 3 these equations are:

$$\dot\phi = p - 0.2311q + 0.093r + 0.0454\phi \quad (4\text{-A-A})$$

$$\dot\psi = 0.3746q + 0.9271r + 0.0193\phi \quad (5\text{-A-A})$$

$$\dot\theta = 0.9555q - 0.3861r + 0.0468\phi + 0.0496\psi \quad (6\text{-A-A})$$

Where it is possible to notice that the terms in ϕ and ψ are small regarding the other terms. In section 4 of this work it will be possible to note how far these terms can be neglected regarding the design procedure. Similar results to those showed in equations (4-A-A), (5-A-A) and (6-A-A) were obtained for other flight conditions. It must be stressed that these terms can be neglected regarding the design procedure, but not regarding the vehicle dynamic response.

So, it is possible to use the following simplified coupled model for the design,

$$\dot x = Ax + Bu \quad (7)$$

where the *A* matrix is given by

$$\begin{bmatrix} 0 & P_{cru}r_0 & P_{cru}q_0 & 0 & 0 & 0 \\ Q_{cru}r_0 & 0 & Q_{cru}p_0 & 0 & 0 & 0 \\ R_{cru}q_0 & R_{cru}p_0 & 0 & 0 & 0 & 0 \\ 1 & -\cos\phi_0 tg\psi_0 & sin\phi_0 tg\psi_0 & 0 & 0 & 0 \\ 0 & sin\phi_0 & \cos\phi_0 & 0 & 0 & 0 \\ 0 & \frac{\cos\phi_0}{\cos\psi_0} & \frac{-sin\phi_0}{\cos\psi_0} & 0 & 0 & 0 \end{bmatrix} \quad (8)$$

the *B* matrix is given by

$$\begin{bmatrix} Cm_\phi & 0 & 0 \\ 0 & Cm_\theta & 0 \\ 0 & 0 & Cm_\psi \\ 0 & 0 & 0 \\ 0 & 0 & 0 \\ 0 & 0 & 0 \end{bmatrix} \quad (9)$$

and the state vector x is simply

$$x^T = \begin{bmatrix} p & q & r & \phi & \psi & \theta \end{bmatrix} \quad (10)$$

the control vector is

$$u^T = \begin{bmatrix} \delta_r & \delta_z & \delta_y \end{bmatrix} \quad (11)$$

with the following parameters defined as

$$P_{cru} = -\frac{(I_{zz} - I_{yy})}{I_{xx}} \quad (12)$$

$$R_{cru} = -\frac{(I_{yy} - I_{xx})}{I_{zz}} \quad (13)$$

$$Q_{cru} = -\frac{(I_{xx} - I_{zz})}{I_{yy}} \quad (14)$$

$$Cm_\phi = \frac{M_\phi}{I_{xx}} \quad (15\text{-a})$$

$$Cm_\theta = \frac{M_\theta}{I_{yy}} \quad (15\text{-b})$$

$$Cm_\psi = \frac{M_\psi}{I_{zz}} \quad (15\text{-c})$$

and the attitudes ϕ_0 , ψ_0 and θ_0 that are the attitudes at the point where the equations have being linearized and the angular velocities, p_0 , q_0 and r_0 are the angular velocities at the point where the equations have being linearized. As can be noticed although this is a linear model it is completely coupled.

2.3 Linear Decoupled Model

It can be also used a linear decoupled model for the design of the control law. In that case the model is simply described by

$$\dot{x}_{dec} = A_{dec} x_{dec} + B_{dec} u_{dec} \quad (16)$$

where A_{dec} is given by

$$\begin{bmatrix} 0 & 0 \\ 1 & 0 \end{bmatrix} \quad (17)$$

for the three modes, that is, roll , yaw and pitch.

B_{dec}^T is given by

$$\begin{bmatrix} Cm_\theta & 0 \end{bmatrix} \quad (18)$$

for the pitch mode

$$\begin{bmatrix} Cm_\psi & 0 \end{bmatrix} \quad (19)$$

for the yaw mode, and

$$\begin{bmatrix} Cm_\phi & 0 \end{bmatrix} \quad (20)$$

for the roll mode.

And the state vector is given by

$$x_{dec}^T = \begin{bmatrix} q & \theta \end{bmatrix} \quad (21)$$

for the case of pitch mode

$$x_{dec}^T = \begin{bmatrix} r & \psi \end{bmatrix} \quad (22)$$

for the case of yaw mode

$$x_{dec}^T = \begin{bmatrix} p & \phi \end{bmatrix} \quad (23)$$

for the case of roll mode, and finally u_{dec} is, δ_z for the pitch mode, δ_y for the yaw mode and δ_r for the roll mode.

3 CONTROL LAW DESIGN

The control law can be designed using the linear coupled model and also using the linear decoupled model. In any case it will be given by,

$$\beta_z = -G_1 q - G_2 \theta + G_2 \theta_{ref} \quad (24)$$

$$\beta_y = -G_3 r - G_4 \psi + G_4 \psi_{ref} \quad (25)$$

$$\beta_r = -G_5 p - G_6 \phi + G_6 \phi_{ref} \quad (26)$$

where θ_{ref} , ψ_{ref} and ϕ_{Refs} are the reference attitudes to be tracked. The β_z is the command input for the relay, (figure 2) in the pitch-channel , β_y is the command input for the relay in the yaw-channel and β_r is the command input for the relay in the roll-channel. It can be noticed that this is not the usual switching function used in this kind of controller. As already known the switching function in general is only a linear combination of (q , θ) for the pitch channel, (r , ψ) for the yaw channel and (p , ϕ) for the roll channel.

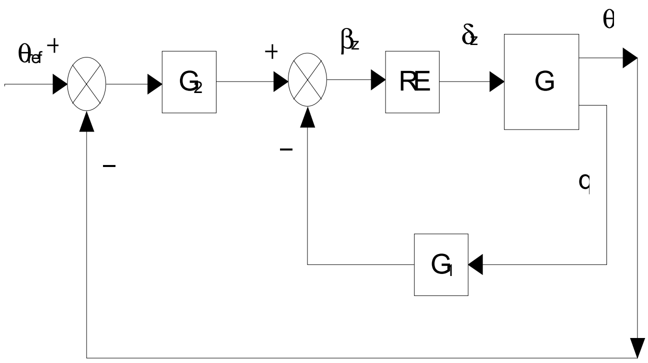

Figure 2- Block diagram of the control law for the pitch-channel.

As the example vehicle used for this study is symmetric with respect to pitch and yaw, the gain G_1 is equal the gain G_3 and the gain G_2 is equal the gain G_4 . All the gains were obtained for the linear decoupled model and for the linear coupled model with the LQR (linear quadratic regulator) technique, as developed for example in Friedland (1987). At this point it is important to say that if the linear decoupled model is used for the design, it will be not necessary to schedule the obtained gains with respect to flight time. This is due to the fact that their calculation is independent of the vehicle trajectory. On the other side, if the linear coupled model is used for the design, it will be necessary to use gain scheduling with respect to flight time. Such scheduling is necessary to achieve an improved performance. This is necessary because the design is based on trajectory dependent parameters. In figure 2, there is the block diagram of the control law for the pitch mode. For the other two modes, the diagram is analogous. In this figure, G represents the vehicle open loop transfer function.

For both cases, with the decoupled linear model or with the coupled linear model the LQR method can be used. The performance index used in the LQR method is given by

$$PI = \int_0^{\infty} (x^T Q x + u^T R u) d\tau \quad (27)$$

where Q is the state weight matrix and R is the control weight matrix.

In the case of the decoupled linear model the state weight matrices were selected as

$$Q_z = \begin{bmatrix} q_q & 0 \\ 0 & q_\theta \end{bmatrix} \quad (28)$$

$$Q_y = \begin{bmatrix} q_r & 0 \\ 0 & q_\psi \end{bmatrix} \quad (29)$$

$$Q_r = \begin{bmatrix} q_p & 0 \\ 0 & q_\phi \end{bmatrix} \quad (30)$$

and the control weights were selected as

$$R_z = \rho_z \quad (31)$$

$$R_y = \rho_y \quad (32)$$

$$R_r = \rho_r \quad (33)$$

In the case of the linear coupled model the state weight matrix was selected as,

$$Q = diagonal(q_p, q_q, q_r, q_\phi, q_\psi, q_\theta) \quad (34)$$

and the control weight matrix was selected as,

$$R = diagonal(\rho_r, \rho_z, \rho_y) \quad (35)$$

The gain vector, K, is obtained by

$$K = R^{-1} B^T P \quad (36)$$

where P is a symmetric and positive definite matrix obtained by solution of the algebraic matrix Riccati equation

$$PA + A^T P + Q - PBR^{-1} B^T P = 0 \quad (37)$$

For the continuous case, the control law is given by

$$u = -Kx \quad (38)$$

Here, the approach used is only to obtain the gain vector to be used in the control logic. In the case of the coupled model the K gain matrix will be a (3x6) matrix. In this case the following gains are used:

$$G_1 = K_{22},\ G_2 = K_{26},\ G_3 = K_{33},\ G_4 = K_{35},$$
$$G_5 = K_{11} \text{ and } G_6 = K_{14}$$

In the case of the decoupled model, only two gains were obtained for each channel, and they are both used. It is important to note that the followed approach, when used with the coupled model, will also give coupled gains. With coupled gains it is possible to study the performance of a control law of the following kind:

$$\beta_r = K_{11}p + K_{12}q + K_{13}r + K_{14}\phi + K_{15}\psi + K_{16}\theta \quad (24\text{-A})$$

$$\beta_z = K_{21}p + K_{22}q + K_{23}r + K_{24}\phi + K_{25}\psi + K_{26}\theta \quad (25\text{-A})$$

$$\beta_y = K_{31}p + K_{32}q + K_{33}r + K_{34}\phi + K_{35}\psi + K_{36}\theta \quad (26\text{-A})$$

This structure is not the usual one, and will be studied in a further research work, in order to study a coupled control logic. With this choice, and with the described models it is then possible to obtain the gains for both cases and each mode. This can be performed very easily with the Control Toolbox function LQR2 of the MATLAB (1987) software.

4 CASE STUDY

A design example was carried out for a satellite launcher vehicle (VLS), using both models, the linear coupled and the linear decoupled. Table 1 reports the vehicle parameters used in the design.

Table 1- Vehicle inertial and control parameters for the design example

I_{yy}	(Kg. m^2)	714.89	M_θ (N.m)	5.224
I_{zz}	(Kg. m^2)	716.43	M_ψ (N.m)	5.224
I_{xx}	(Kg. m^2)	154.06	M_ϕ (N.m)	1.874

The weights used in the design are reported in table 2. These weights were obtained by simulation using as a first approach the linear decoupled model, that is, simulating and noting if the system response satisfies the desired performance, that is, a good tracking performance.

In table 3 the trajectory point used in the linearization of the linear coupled model is reported.

In table 4 the gains obtained for each design are shown. From here on, the control law designed based on the decoupled model, will be called CL1 control law, and the control law designed based on the coupled model will be called CL2

Table 2 - Weights used in the performance index to obtain the control law gains

q_p	1	q_q	1	q_r	1
q_ϕ	1	q_θ	1	q_ψ	1
ρ_r	0.1	ρ_z	0.1	ρ_y	0.1

Table 3 - Trajectory point used for linearization of the non-linear model

ϕ_0	22°	θ_0	-57°	ψ_0	14°
p_0	6°/sec	q_0	2°/sec	r_0	2°/sec

Table 4 - Gains obtained for each design

CL1 control law		CL2 control law	
Decoupled Model		Coupled Model	
Pitch-Mode		Pitch-Mode	
G_1	29.5888	G_1	79.291
G_2	3.1623	G_2	21.624
Yaw-Mode		Yaw-Mode	
G_3	29.588	G_3	78.083
G_4	3.1623	G_4	22.020
Roll-Mode		Roll-Mode	
G_5	23.016	G_5	55.871
G_6	3.1623	G_6	18.914

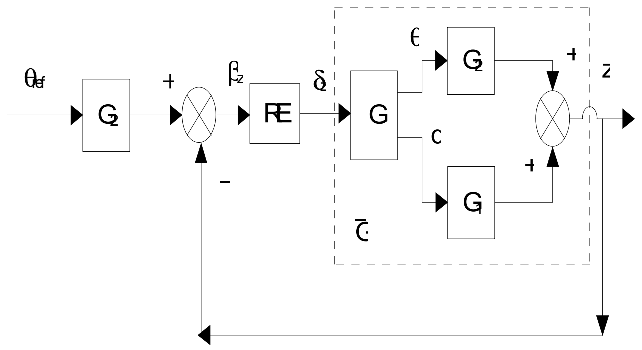

Figure 3 - Simplified block diagram of the control law with the transfer function of the linear part to be used in the stability analysis

control law. From this table it can be noticed that the CL2 design will require much more control effort, which in this case, means that the controller will use more gas than the CL1 controller.

In figure 3 there is a simplified block diagram of figure 2, which shows the transfer function $\bar{G}$ of the linear part to be used in the stability analysis and limit cycle analysis.

In table 4A there is a comparison between the calculated gains when the coupled model represented by equations (8) and (9) are used and when the complete coupled model given by equations (1-A) to (6-A) is used. As can be noticed the used model is quite good for the design.

Table 4A- Gains Comparison

CL2 control law		CL2 control law	
Coupled Model		Complete Coupled Model	
Pitch-Mode		Pitch-Mode	
G_1	79.291	G_1	80.555
G_2	21.624	G_2	21.824
Yaw-Mode		Yaw-Mode	
G_3	78.083	G_3	77.997
G_4	22.020	G_4	21.899
Roll-Mode		Roll-Mode	
G_5	55.871	G_5	56.047
G_6	18.914	G_6	19.219

In this figure z is defined as the following vector:

$$z = \begin{bmatrix} G_1 & G_2 \end{bmatrix} \begin{bmatrix} q \\ \theta \end{bmatrix}$$

The transfer functions of the linear part of each control law for each mode are given by equations (39,40,41) for the linear decoupled model, and by equations (42,43,44) for the linear coupled model.

$$\bar{G}_\theta = \frac{0.216s + 0.0231}{s^2} \qquad (39)$$

$$\bar{G}_\psi = \frac{0.216s + 0.0231}{s^2} \qquad (40)$$

$$\bar{G}_\phi = \frac{0.2808s + 0.0386}{s^2} \qquad (41)$$

$$\bar{G}_\theta = \frac{0.578s^2 + 0.1514s + 0.0043}{s^3 + 0.0068s} \qquad (42)$$

$$\bar{G}_\psi = \frac{0.57s^2 + 0.1497s + 0.0044}{s^3 + 0.0068s} \qquad (43)$$

$$\bar{G}_\phi = \frac{0.6816s^3 + 0.2308s^2 + 0.0037s + 0.0019}{s^4 + 0.0068s^2} \qquad (44)$$

In equations (39) to (44) the symbol s is meaning the Laplace operator.

5 LIMIT CYCLE ANALYSIS

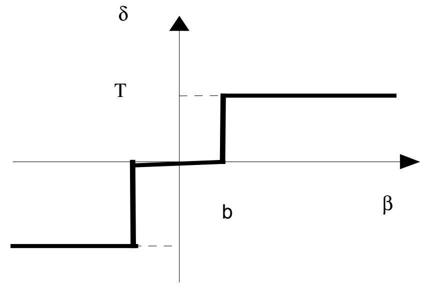

Figure 4 - Diagram of the relay characteristics used in the control system.

In order to verify if the system will be subject to a limit cycle, the use of the describing function technique for a relay with dead zone was used. Such technique can be found in several references, as Gibson (1963) , Greensite (1970) and others. Here, in particular, the notation of Van de Vegte (1990) is used. The describing function for the relay can be obtained for example from Van de Vetge, and is given by

$$N = \frac{4T}{\pi A}\sqrt{1 - \frac{b^2}{A^2}} \qquad (45)$$

where b is the dead zone, and T is the relay output, as showed in figure 4. In equation (45) A is the amplitude of the sinusoidal input to the relay, so N will be a function of this amplitude.

In the design example the dead zone was used as 0.1 ,that is, $b = 0.1$. This value was obtained by simulation of both control laws, as the one that gives the best performance. The relay output T was taken as $T = 1$. The plotting of $-1/N(A)$ and of $\bar{G}(iw)$ for each transfer function has shown that there is no interception between the curves in any case. With this result the describing function technique does not foresee any limit cycle, in this preliminary study. However, as can be seen in the simulations a limit cycle will occur in the system.

The limit cycle is noticed not only in the digital simulations, but also in the hybrid simulations with a usual controller. The existence of a limit cycle for this kind of controller is also addressed in Bryson. A more detailed analysis can be performed in a future study, by including the actuator model. These inclusions have not been made here because the work was developed as a preliminary research to investigate the general performance of this kind of controller, since it is not the usual controller for the problem addressed.

6 STABILITY ANALYSIS

For the stability analysis of the control system the Circle criterion was used. Here, the Popov criterion cannot be used because the transfer functions of the linear part do not have all the poles to the left of the s-plane. The Circle criterion can also be found in several books about non-linear control, here in particular, the notation adopted by Tsypkin (1984) and by Brogan (1991) was used. As the dead zone used was 0.1 and the relay output T= 1, it results that the plot of $\bar{G}(iw)$ must lie to the right of the vertical line passing by-0.1 in the s-plane. The plots of the transfer functions have shown that they lie to the right of -0.1 only above certain frequency.

The plotting of $\bar{G}_\theta$ for the linear decoupled case lies to the right of -0.1 only for frequencies above 0.48 rad/sec. The plotting of $\bar{G}_\theta$ for the linear coupled case lies to the right of -0.1 only for frequencies above 1.23 rad/sec. The results for the plotting of $\bar{G}_\psi$ are analogous. The plotting of $\bar{G}_\phi$ for the linear decoupled case lies to the right of -0.1 only for frequencies above 0.62 rad/sec. The plotting of $\bar{G}_\phi$ for the linear coupled case lies to the right of -0.1 only for frequencies above 1.52 rad/sec. So in view of these facts it can be said that the design based on the linear decoupled model shows a large band of stability than the design based on the coupled model. Here again a more detailed analysis will be performed in future studies, with the inclusion of the actuator model.

7 FLYING QUALITIES STUDY

The flying qualities of the vehicle with the designed control laws were assessed in order to obtain which one will be the most suitable design to be used. The effects of dead-zone, tracking, regulation and decoupling responses were studied.

7.1 Dead Zone Effect

In figure 5A there is the pitch-attitude response for a commanded pitch-attitude step of 5.73°. The results were obtained from the simulation of the non-linear model working with the CL1 control law for the relay without dead-zone and for the relay with dead-zone. It can be noticed that in this case the dead-zone influence is very important, and the vehicle performance is very degraded. In figure 5B the same response is shown for the CL2 control law. It can be noticed that in this case the dead-zone influence is not very important, and the vehicle performance is not very degraded with respect to the ideal performance.

If one uses CL1 with the linear decoupled model, and CL2 with the linear coupled model, these effects cannot be observed. They appear more probably due to the non-linear and coupling effects of the real model.

7.2 Tracking Performance

To assess the control law performance with respect to tracking, the time responses obtained from the non-linear model simulation working with CL1 and with CL2 were compared. Here in all cases it was considered a 0.1 dead-zone. In figure 6A the roll-attitude response for a commanded roll-attitude step of 5.73° obtained with the CL1 control law and with the CL2 control law is reported. It can be noticed that the vehicle working with the CL2 control law offers a better performance.

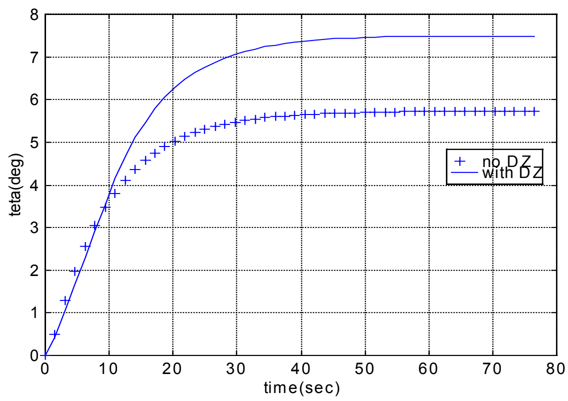

Figure 5A - Pitch-attitude response for a commanded pitch-attitude step (5.73°) obtained with CL1 without and with dead-zone.

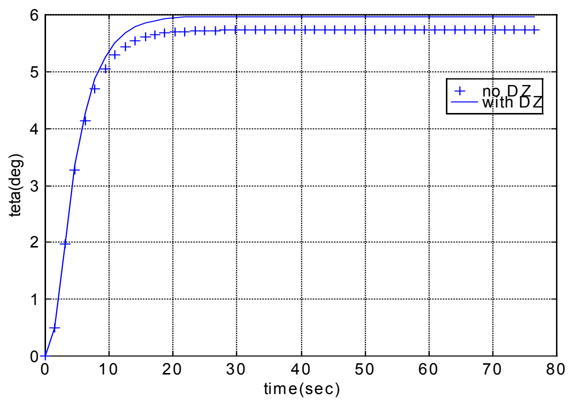

Figure 5B - Pitch-attitude response for a commanded pitch-attitude step (5.73°) obtained with CL2 without and with dead-zone.

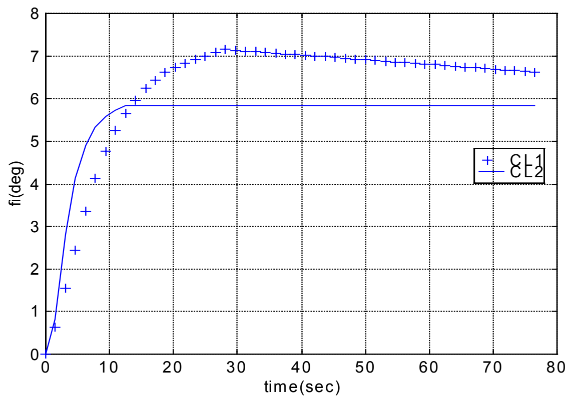

Figure 6A - Roll-attitude following a 5.73° commanded roll-attitude step obtained with CL1 and with CL2.

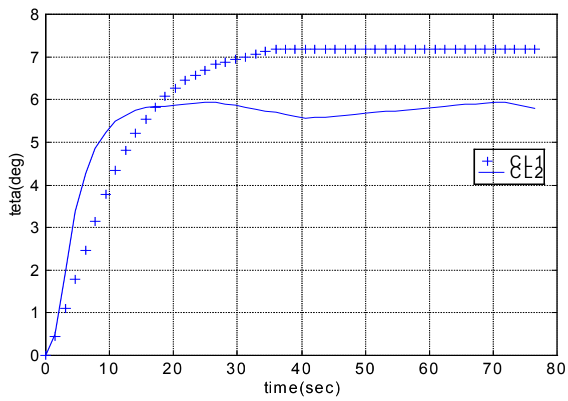

Figure 6B - Pitch-attitude following a 5.73° commanded pitch-attitude step obtained with CL1 and with CL2.

In figure 6B the pitch-attitude response for a commanded pitch-attitude step of 5.73° obtained with the CL1 control law and with the CL2 control law is reported. It can be noticed that the vehicle working with the CL2 control law offers again a better performance. The yaw response is similar to the pitch-response due to the symmetric characteristics of the vehicle.

This fact was already expected, since CL2 was designed based on a coupled model, whereas CL1 was designed based on a

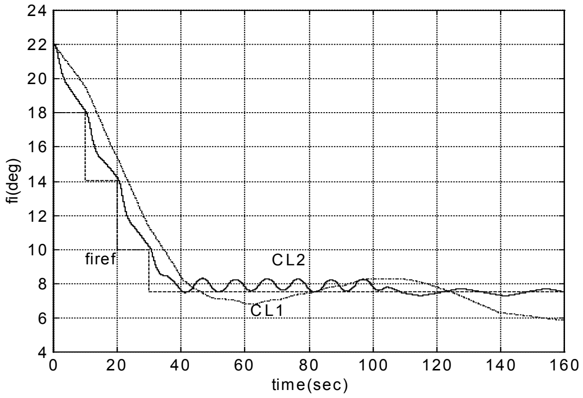

Figure 7A - Roll-attitude following a simultaneous commanded roll and pitch attitude, obtained with CL1 and with CL2.

.

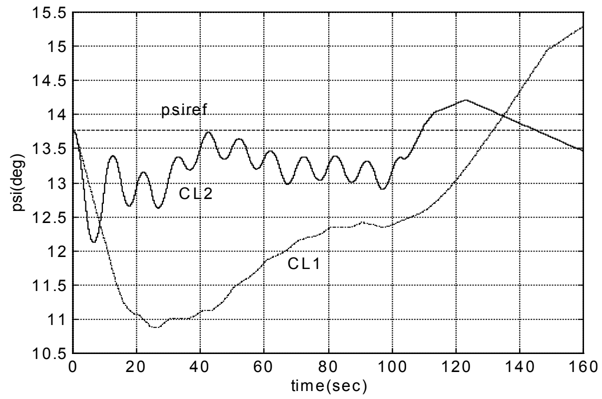

Figure 7B - Yaw-attitude following a simultaneous commanded roll and pitch attitude, obtained with CL1 and with CL2.

complete decoupled model. This same behaviour was already seen in the design of continuous controllers, as in Oliva & Leite (1998).

In figure 7A, 7B and 7C the attitude responses are shown for a manoeuvre starting with zero angular velocities, and the following initial attitudes: $\phi = 22°$, $\psi = 13.7°$, $\theta = -57°$, that represent actual vehicle attitudes, and actual vehicle manoeuvres. The commanded attitudes are showed in these figures, with their final values given by $\phi = 7.7°$, $\psi = 13.7°$, $\theta = -120°$, that is, there is a simultaneous roll and pitch manoeuvre, with fixed yaw attitude.

From these figures (7A and 7C) it is clear again that CL2 can give a better tracking performance than CL1, and a much better decoupling performance than CL1(centre).

7.3 Regulation Performance

To assess the regulation performance of both control laws, a non-linear simulation of the vehicle working with CL1 and with CL2 was carried out for the following initial conditions:

$\phi = 22°$, $\psi = 13.7°$, $\theta = -57°$, $p = 5°/s$, $q = 5°/s$, $r = 5°/s$.

In all cases it was considered 0.1 dead-zone.

In figure 8A there is the roll-attitude response where it is possible to notice that CL1 is showing a better performance than CL2.

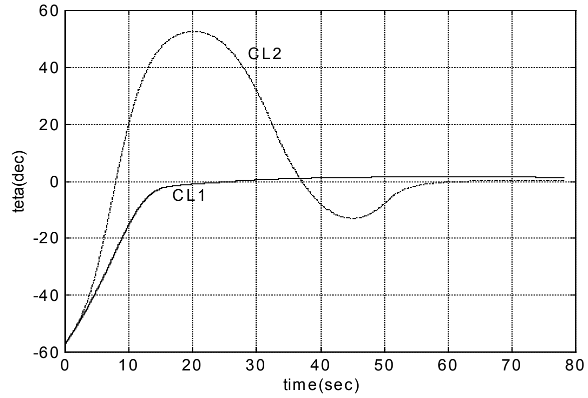

Figure 8 - Pitch-attitude response with CL1 and CL2, for an initial condition in pitch.

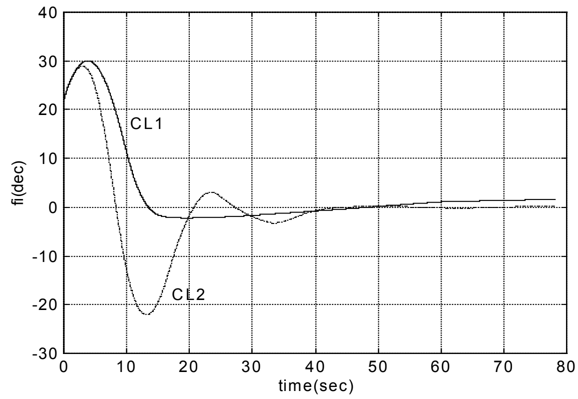

Figure 8A - Roll-attitude response with CL1 and CL2, for an initial condition, in roll.

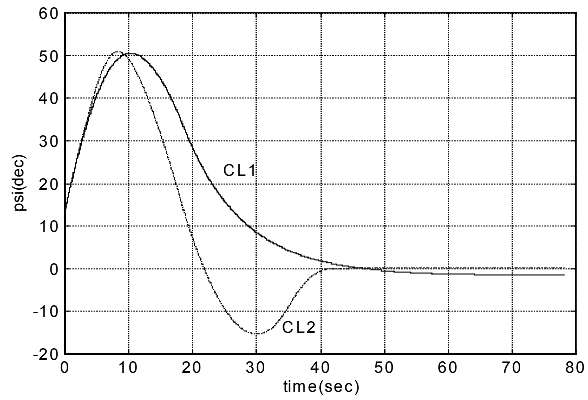

Figure 8B - Yaw-attitude response with CL1 and CL2, for an initial condition in yaw.

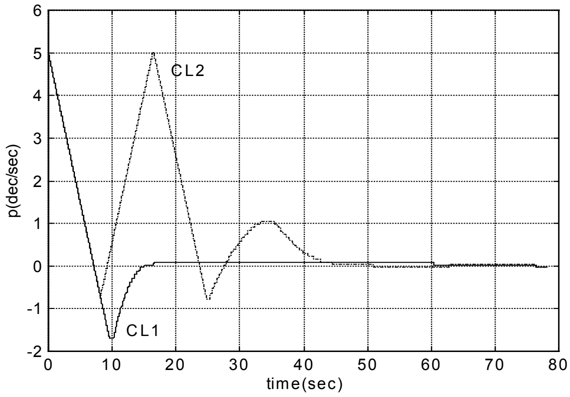

Figure 9A - Roll-rate response with CL1 and CL2 for an initial condition in roll-rate.

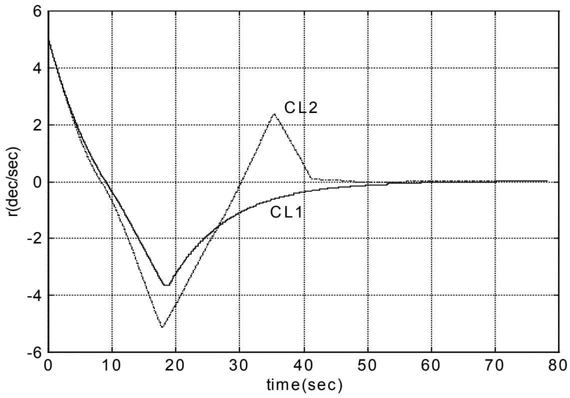

Figure 9B - Yaw-rate response with CL1 and CL2 for an initial condition in yaw-rate.

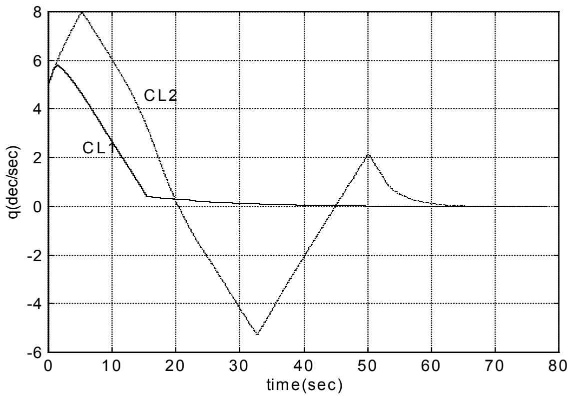

Figure 9C - Pitch-rate response with CL1 and CL2 for an initial condition in pitch-rate.

In figure 8B there is the yaw-attitude response. Here again it is possible to notice that CL1 is showing a performance much better than CL2.

In figure 8C there is the Pitch-attitude response, and in this case it is also possible to notice that CL1 is showing a performance much better than CL2.

In figures 9A, 9B and 9C the angular velocities responses are shown, and in all three cases the regulation performance given by CL1 is much better than that given by CL2. This was already expected, since the obtained gains for CL1 were smaller than those obtained for CL2. In view of this certainly CL1 will be more suitable to do system regulation.

8 ROBUSTNESS PERFORMANCE

The robustness performance was assessed with respect to uncertainty on the control moments, roll, pitch and yaw, and also with respect to uncertainty on the inertial moments. A 10% uncertainty was considered for the control moments.

In figure 10A it is reported the roll-attitude response for a 5.73° commanded roll-attitude step (5.73°). The responses are for the CL2 control law without uncertainty in the control forces and with 10% uncertainty in the control forces. It can be noticed that the performance is practically not affected by such uncertainty.

In figure 10B it is reported the Pitch-attitude response for a

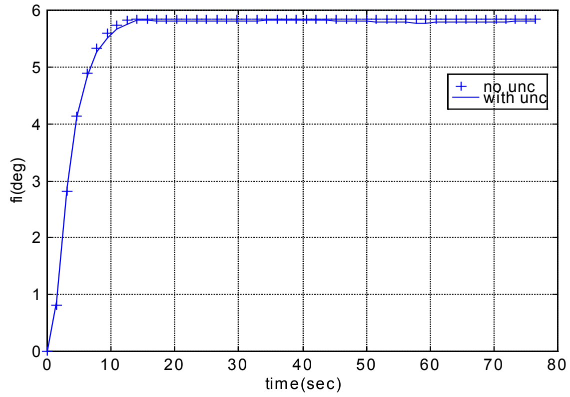

Figure 10A - Roll-attitude following a 5.73° step commanded roll-attitude, without and with uncertainty in the control forces. All for CL2 control law.

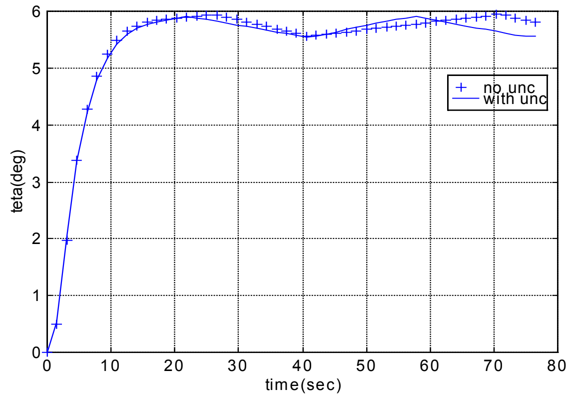

Figure 10B - Pitch-attitude following a 5.73° step commanded pitch-attitude without and with uncertainty in the control forces. All for CL2 control law.

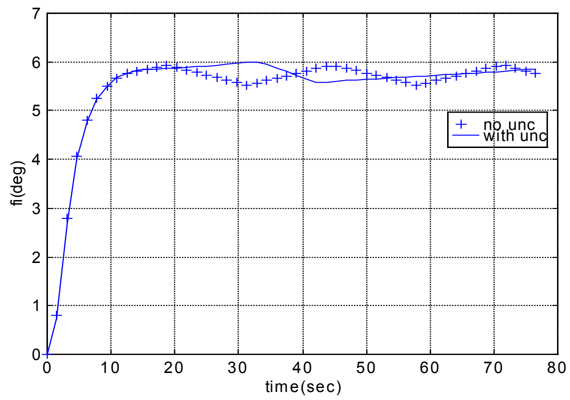

Figure 10C - Roll-attitude following a 5.73° step commanded roll-attitude without and with uncertainty in the inertial parameters. All for CL2 control law.

5.73° commanded Pitch-attitude step for the CL2 control law without uncertainty and with 10% uncertainty in the control forces. Here again it is noticed that the uncertainty effect is negligible on the system performance.

In figure 10C it is reported the roll-attitude response for a commanded 5.73° roll-attitude step for the CL2 control law without uncertainty and with 10% uncertainty in the inertial parameters. Here again it is noticed that the uncertainty effect is negligible on the system performance.

This shows that optimal control systems are quite robust. However future studies must be performed with simultaneous manoeuvres and both uncertainties working together, in order to get a more realistic picture of the case.

9 DECOUPLING PERFORMANCE

For a complete decoupled system, when the vehicle performs, for example, a roll and yaw manoeuvre simultaneously, the pitch attitude response is expected to be zero.

In figure 11A it is reported the pitch-attitude response obtained with both control laws, CL1 and CL2, when the vehicle performs a simultaneous step manoeuvre in yaw and roll.

In the same way, a complete decoupled system will give a zero roll-attitude response when the vehicle performs a simultaneous yaw and pitch manoeuvre. In figure 11B it is shown the roll-attitude response for both control laws, CL1 and CL2, when the vehicle performs a simultaneous pitch and yaw step manoeuvre.

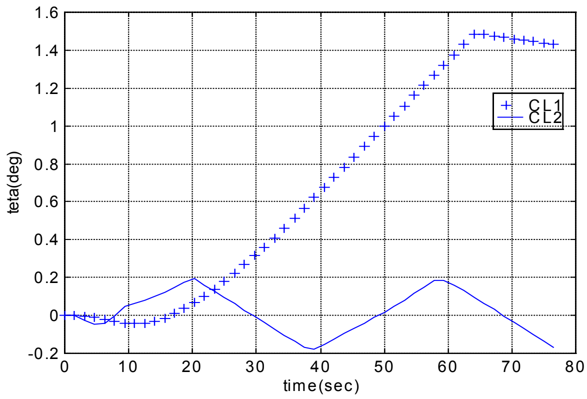

Figure 11A -Pitch-attitude response following a simultaneous yaw and roll step manoeuvre of 5.73° with CL1 and with CL2

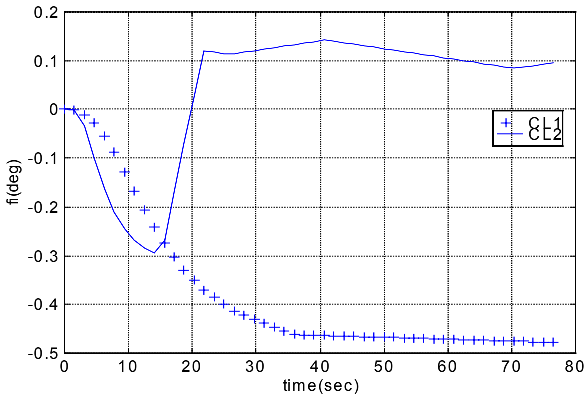

Figure 11B - Roll-attitude response following a simultaneous yaw and pitch step manoeuvre of 5.73° with CL1 and with CL2.

From this figure it can be noticed that the control law CL2 clearly offers a much more decoupled response. The decoupling degree can even be better with an appropriate redesign of the CL2 gains by iterating on the weight matrices Q and R, or using these gains scheduled with time. An appropriate redesign of CL1 can also improve the CL1 performance, but never with the same degree obtained by CL2. This was already expected, since CL2 is designed based on a coupled model, whereas CL1 is based on a decoupled model. This can also be verified in Oliva & Leite (1998) for the continuous controller design.

10 GENERAL PERFORMANCE

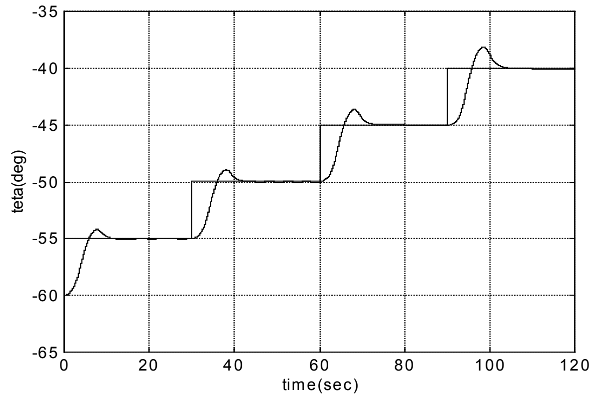

Figure 12A - Pitch-attitude CL2 response following a simultaneous yaw, pitch and roll manoeuvre.

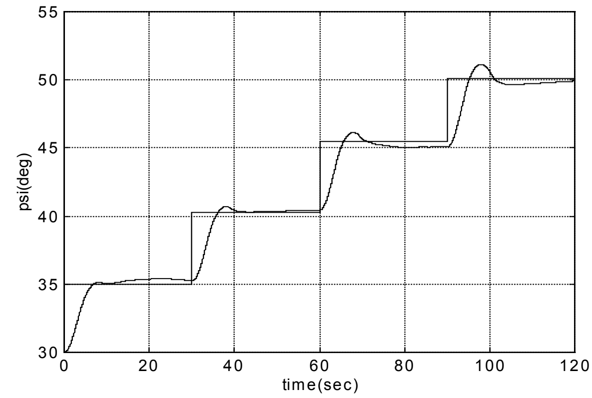

Figure 12B - Yaw-attitude CL2 response following a simultaneous yaw, pitch and roll manoeuvre.

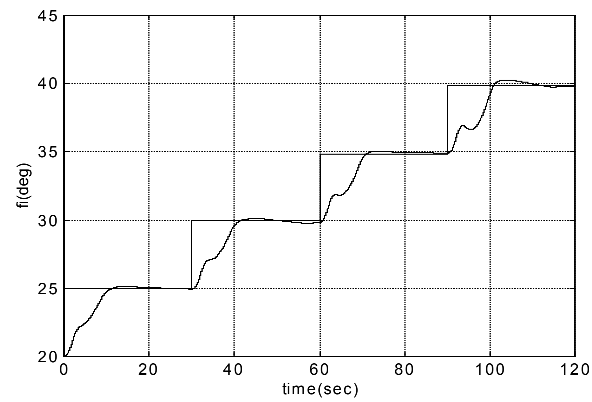

Figure 12C - Roll-attitude CL2 response following a simultaneous yaw, pitch and roll manoeuvre.

In the preceding sections the system performance was assessed in some cases starting the simulations with zero initial conditions. For non zero initial conditions it is necessary first to bring the angular velocities to zero, and then after this, it is possible to perform the manoeuvre with non zero initial attitude conditions. This was necessary in order to get a better performance. If the vehicle starts the manoeuvre with initial angular velocities, it is starting the manoeuvre with inertial coupling, so bring the angular velocities to zero will make the inertial coupling zero at the beginning. This is also the procedure applied for the common used controller, that carries the manoeuvre one by one, that is, plane by plane. However, the manoeuvre must be performed in steps, or in a smooth path, that is, for large amplitudes manoeuvres the system will keep decoupling between the responses only if the manoeuvre is smooth. In figures 12A,12B and 12C the time histories for a simultaneous manoeuvre in pitch, yaw and roll, for large angles are shown. As can be noticed the tracking and decoupling is quite good. Although these figures show 120 seconds to the system reach the new condition, it can be noticed that half of this time will be enough, since each step can be attained in 10 seconds.

In figures 13A, 13B ,13C , 14A, 14B and 14C a typical pointing manoeuvre is showed, for the system working the first 70 seconds with CL1 and the remaining time with CL2. The system initial conditions are the following:

$\phi = 22°$, $\psi = 13.7°$, $\theta = -57°$, $p = 6°/s$, $q = 2°/s$, $r = 2°/s$.

The system final commanded conditions are the following:

$\phi = 7.5°$, $\psi = 13.7°$, $\theta = -120°$

In the first 70 seconds the angular velocities are driven to zero, in order to make the inertial coupling zero. Then in the remaining time the attitude manoeuvre is performed. It can be noticed that the manoeuvre is well done, and with a good

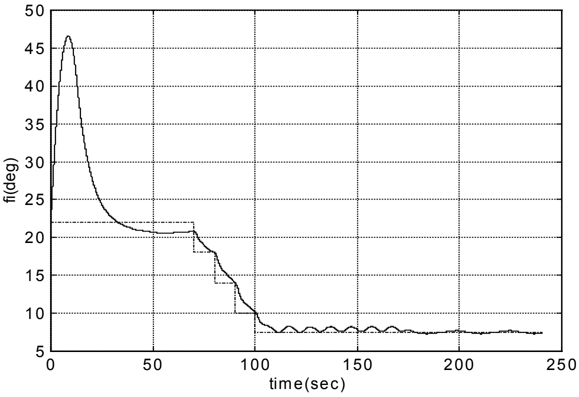

Figure 13A - Roll-attitude response for a typical pointing manoeuvre

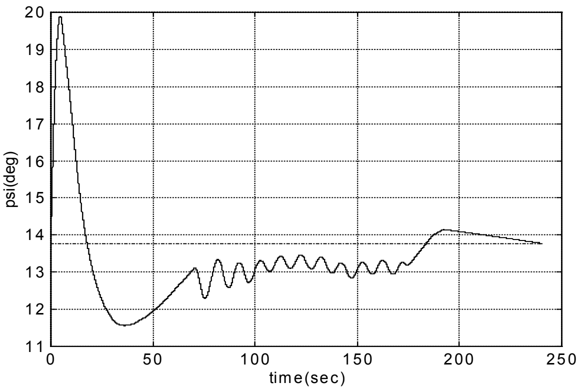

Figure 13B - Yaw-attitude response for a typical pointing manoeuvre.

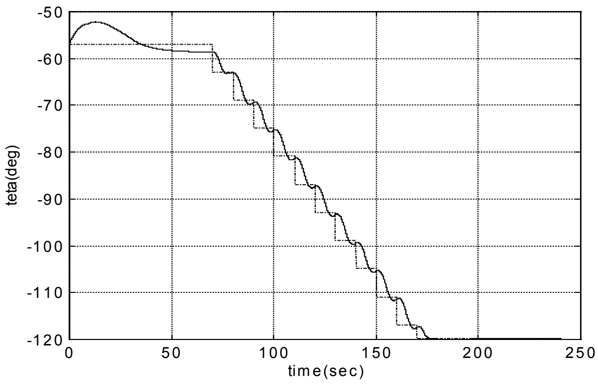

Figure 13C - Pitch-attitude response for a typical pointing manoeuvre

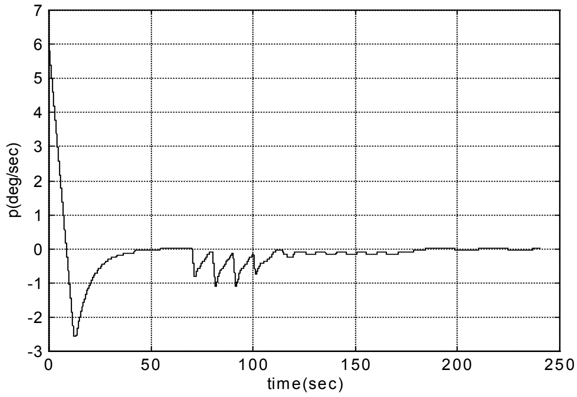

Figure 14A - Roll-rate response for a typical pointing manoeuvre.

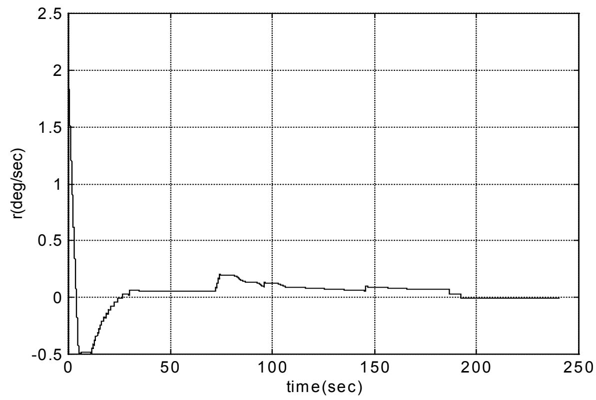

Figure 14B -Yaw-rate response for a typical pointing manoeuvre

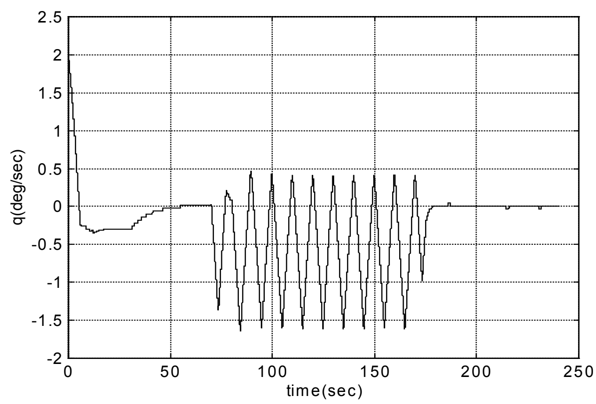

Figure 14C - Pitch-rate response for a typical pointing manoeuvre.

Table 5 - Gas Consumption Necessary to Perform each Manoeuvre

	Tracking Manoeuvre		Regulation Manoeuvre	
	CL1	CL2	CL1	CL2
Roll (N.s)	6.43	17.93	45.12	62.56
Yaw (N.s)	4.03	11.12	49.37	80.37
Pitch (N.s)	4.18	11.25	60.81	94.18
Total (N.s)	14.65	40.31	155.31	242.12

performance. It is also possible to notice the limit cycles in figures 14A, 13B and 14C. They were not predicted by the describing function technique, since there, a very simple model was used, and here the vehicle is represented by its non-linear model. It is useful to remember, that for example, $\dot{\psi} = r$ only for a complete decoupled model. In figure 13B one can notice yaw angle oscillations, whereas in figure 14B there are almost no yaw rate. In the non-linear case the yaw oscillations are given by equation (5). The yaw angle oscillations in figure 13B are consequences of the pitch-rate in figure 14C and yaw-rate in figure 14B. One can also notice the limit cycle occurring in the same time window, around 70 to 170 seconds. In figures 15A, 15B and 15C the phase-plane plots for a typical pointing manoeuvre are shown. In this figure a stable limit cycle is clearly noticed. The limit cycle showed in figures 14A, 13B and 14C was not predicted by the very simple analysis of the describing function. Even when the vehicle is working with only one control law (CL1 or CL2) during all the manoeuvre time this limit cycle is also present. It is also present without time delay. The limit cycle is mainly a function of the magnitude of the gains and the flight condition when the manoeuvre starts. For the vehicle working only with CL1 a limit cycle with lower amplitude is present, and for the vehicle working with CL2 a limit cycle with higher amplitude is present. There are however, flight conditions when there are no limit cycle oscillations. The kind of manoeuvre that the vehicle performs will also play a major role on the presence or not of the limit cycle.

11 GAS CONSUMPTION PERFORMANCE

In table 5 the gas consumption necessary to accomplish each manoeuvre is reported. It is quite clear that the CL1 design requires much less gas consumption to perform the manoeuvre than the CL2 control law. However the values required by the CL2 control law are still acceptable with respect to a real implementation.

12 CONCLUSIONS AND COMMENTS

In conclusion it is important to stress that the CL2 design depends on trajectory parameters, while the CL1 design does not. The simulation results showed that both designs are subjected to a limit cycle, although the describing function technique did not preview such limit cycle. It can be concluded that the describing function technique is not appropriate to study a limit cycle existence on this kind of system. As one can see even a very simple analysis as described in Bryson can preview that existence. On the other side, with respect to the Circle criterion CL1 shows better stability characteristics than CL2, what is ratified in the regulation performance studies. It was noted that the dead-zone is much more influent in the CL1 design, while for the CL2 design it practically does not matter. The tracking performance given by CL2 design is clearly much better than the one given by the CL1 design. It was noticed that CL2 has a good robustness degree with respect to uncertainties. It was also quite clear that the decoupling performance given by CL2 is much better than that given by CL1.

Finally the gas consumption performance given by CL1 is much better than that given by CL2, what was expected, since the gain's magnitude of CL1 were much lower than those of CL2. Certainly the CL2 performance can be improved with an appropriate redesign of its gains, by iterating in the weight matrices *Q* and *R* and observing the obtained responses. For an appropriate system performance it is necessary first to bring the angular velocities to zero, and then performing the desired manoeuvre in smooth steps. By the end it is better to use a

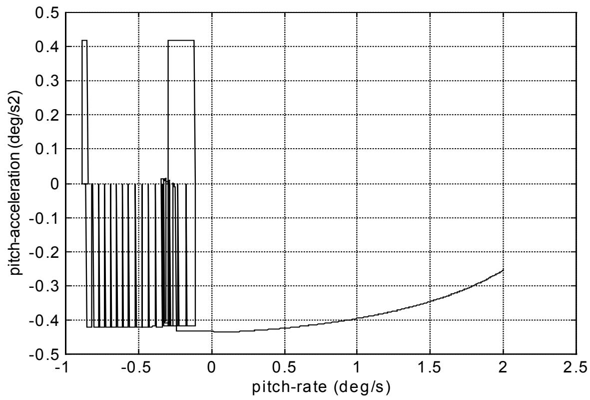

Figure 15A - Phase-Plane plot for *q* versus $\dot{q}$ for a typical pointing manoeuvre.

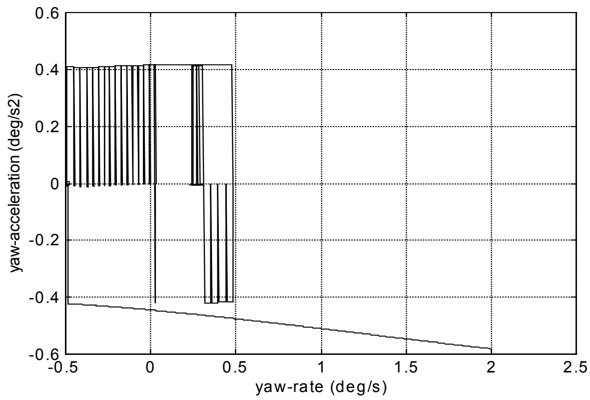

Figure 15B - Phase-Plane plot for *r* versus $\dot{r}$ for a typical pointing manoeuvre.

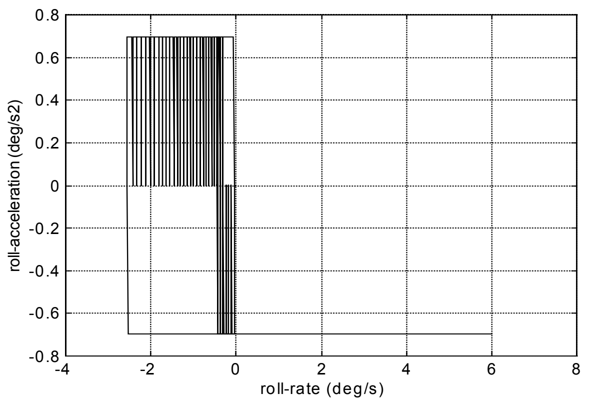

Figure 15C - Phase-Plane plot for *p* versus $\dot{p}$ for a typical pointing manoeuvre.

combined control law to perform a pointing manoeuvre, as showed in figures 13 and 14. This combined control law uses CL1 to work as a regulator and CL2 to work as a tracker decoupling. As a final conclusion, the work showed that the structure and approach could be further studied with more details in order to obtain a much better picture of the controller performance.

REFERENCES

Atherton, D.P. (1975). Nonlinear Control Engineering. Van Nostrand Reinhold Co. , New York, 1975.

Boyle, A.J. and Brogan, W.L. (1986). A Nonlinear Controller. Int. Journal of Control. December. Vol.44, No.5, pp. 1209-1218.

Brogan, W.L. (1991). Modern Control Theory. 3rd ed. Prentice Hall. Englewood Cliffs. New Jersey.

Brumann, W.T. and Rugh, W.J. (1986). Feedback Control of Nonlinear Systems by Extended Linearization. IEEE Transactions on Automatic Control. January. Vol. AC-31, No.1 , pp. 40-46.

Bryson, A.E. Jr. (1994). Control of Spacecraft and Aircraft.Princeton University Press. Princeton. New Jersey.

Friedland, B. (1987). Control System Design - McGraw Hill.New York.

Gibson, J.E. (1963). Non-linear Automatic Control.McGraw-Hill Book Company. New York.

Greensite, A.L. (1970). Elements of Modern Control Theory. Vol I : Control Theory. Spartan Books, New York.

Hughes, P.C. (1986). Spacecraft Attitude Dynamics. John Wiley. New York.

Isidori, A. (1985). Nonlinear Control Systems : An Introduction. Springer-Verlag, Berlin.

Moler, C.J. Little, and S. Bangert, (1987). PC-Matlab. The Mathworks, Inc, 20 North Main St, Suite 250, Sherborn, MA 01770.

Oliva, A.P. and Leite Filho, W.C. (1998). A Study about a Control Law that Tracks a Reference Attitude and Maintains Attitude Decoupling. 12th CBA - Brazilian Congress on Automatic Control. Uberlandia- MG - Brazil. - Vol 5 , pp. 1587-1592.

Van de Vegte, J. (1990). Feedback Control Systems, 2nd ed. Prentice Hall, Inc. Englewood Cliffs. New Jersey. Chapter 14, pp. 399-420.

Ya. Z. Tsypkin (1984). Relay Control Systems. Cambridge University Press.